Electronic Supplementary Material (ESI) for Journal of Materials Chemistry B.
This journal is © The Royal Society of Chemistry 2023

Multiple organelle-targeted [1,8]-naphthyridin derivatives for detecting the polarity of organelle

Hao-Chi Hao,[a] Gang Zhang,[b] Ru Sun,[*,a] Yu-Jie Xu,[b] Jian-Feng Ge[*,a, c]

[a] *College of Chemistry, Chemical Engineering and Material Science, Soochow University, 199 Ren'Ai Road, Suzhou 215123, China.*

[b] *State Key Laboratory of Radiation Medicine and Protection, School of Radiation Medicine and Protection and Collaborative Innovation Center of Radiation Medicine of Jiangsu Higher Education Institutions, Soochow University, Suzhou 215123, China.*

[c] *Jiangsu Key Laboratory of Medical Optics, Suzhou Institute of Biomedical Engineering and Technology, Chinese Academy of Sciences, Suzhou 215163, China.*

Index

[*] *Corresponding authors. E-mail addresses: sunru924@hotmail.com (R. Sun), ge_jianfeng@hotmail.com (J.-F. Ge).*

Experimental section

Preparation of the test solution

For the optical assay, the stock solution of dyes **1a-1d** (1 mM) were prepared in 10 mL DMSO. UV-vis absorption and fluorescence emission spectra of **1a-1d** in different solvents including water (H_2O), methanol (MeOH), ethanol (EtOH), dimethyl sulfoxide (DMSO), dichloromethane (DCM), 1,4-dioxane (DiO), and toluene (TOL) with decreasing orientation polarizability (Δf) were recorded. The 100 μL of dyes stock solution was transferred to 10 mL volumetric flasks, and diluted with corresponding solvent to scale line, then mixed. The polarity-response test solutions were prepared from the 100 μL dyes stock solution and the water-dioxane mixed system. Furthermore, the volume percentages of water in the mixed system were 0 %, 10 %, 20 %, 30 %, 40 %, 50 %, 60 %, 70 % and 80 % in turn. As for the pH assay, test solutions of dyes **1a-1d** with different pH values were prepared by mixing 1.0 mL of dyes stock solution (100 μM) with 2.0 mL of DMSO, and then adjusting the volume to 10 mL with PBS. The concentration of test solutions was 10 μM in all optical experiments.

For the photostability experiment, dyes **1a-1d** were dissolved in acetonitrile with a concentration of 10 μM. The acetonitrile solutions of dyes **1a-1d** were continuously irradiated with 500 W of Philips iodine-tungsten lamp for 6 h. Meanwhile, the distance between the irradiated sample and the lamp remains 25 cm, and an 8 cm thick cold trap prepared by $NaNO_2$ (60 g/L) was placed between them in order to eliminate the interference of heat and short wavelength light. During the photostability experiment, the absorbance of the absorption maximum at different times was recorded, and the remaining absorbance (%), a parameter reflecting the trend of photostability, was calculated according to the recorded change of absorbance.

Determination of the relative fluorescence quantum yield

The relative fluorescence quantum yields were measured using the following equation:

$$\Phi_x/\Phi_{st} = [A_{st}/A_x]\,[n_x^2/n_{st}^2]\,[D_x/D_{st}]$$

where st is the standard; x is the sample; F is the quantum yield; A is the absorbance at the excitation wavelength; D is the area under the fluorescence spectra on an energy scale; and n is the refractive index of the solution. Coumarin-153 (Φ = 0.547 in ethanol) was used as the standard.

Cell culture and imaging methods

HeLa cells were cultured with high glucose DMEM supplemented with 10% calf serum and 1% double antibody (penicillin/streptomycin). All cells were cultured in a 5 : 95 CO_2–air incubator at 37 °C. The cytotoxicity of dyes **1a**-**1d** was verified by the CCK-8 method. 10 mL of dyes **1a**-**1d** of

different concentrations (0 μM, 2 μM, 4 μM, 6 μM, 8 μM and 10 μM) were added to the plate respectively and cultured in an incubator for 6 h. Then 10 mL of CCK-8 solutions were added into each plate and incubated for 1 h in the incubator. The formula for calculating the cell survival rate is as follows: Survival rate (%) = $(A_{sample} - A_b)/(A_c - A_b)$, where A_b is the blank (including test substance and media, no cells) and A_c is the negative control (including media and cells, no test substance). For the colocalization imaging experiments, the HeLa cells were co-cultured by dye **1a** (3 μM), **1b** (5 μM), **1c** (10 μM) and **1d** (10 μM) respectively with the corresponding commercial organelle markers including mitochondria (Mito Tracker Red CMXRos, 3 μM), lipid droplets (Nile Red, 50 nM), lysosomes (Red LysTracker, 1 μM) and endoplasmic reticulum (Red ERTracker, 1 μM). In the imaging experiments of cell polarity response, the HeLa cells were incubated with dye **1a** (10 μM), **1b** (5 μM), **1c** (10 μM) and **1d** (10 μM), respectively, and the corresponding drugs that induced cell polarity variations, including nystatin (10 μM), lipopolysaccharide (LPS, 50 μg/mL), DMSO (10 μL) and tunicamycin (500 μg/mL). For Red Tracker, red channel images were obtained from 600 nm to 750 nm when excited at 561 nm. For **1a**-**1d**, green channel images were obtained from 500 nm to 575 nm when excited at 488 nm.

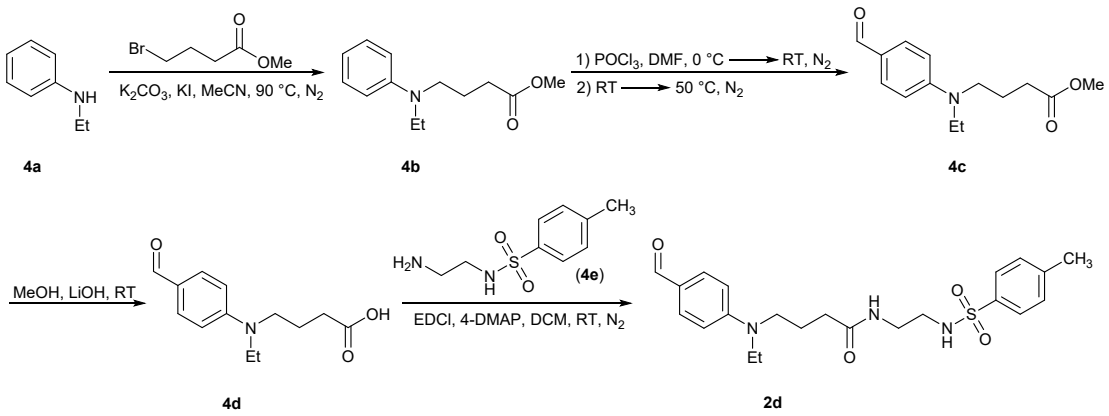

Scheme S1. The synthetic route of compounds **4d** and **2d**.

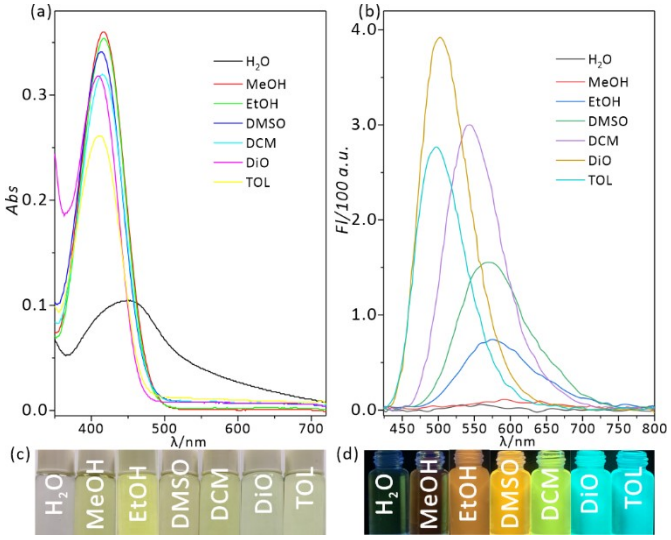

Fig. S1 Spectral properties of dye **1b** (10 μM) in different solvents. (a) UV-visible absorption spectrogram; (b) Fluorescence emission spectrogram (λ_{ex} = 414 nm, slit widths: 1.5 nm/3 nm); (c) photographs in daylight; (d) UV photographs under a 365 nm lamp and darkroom.

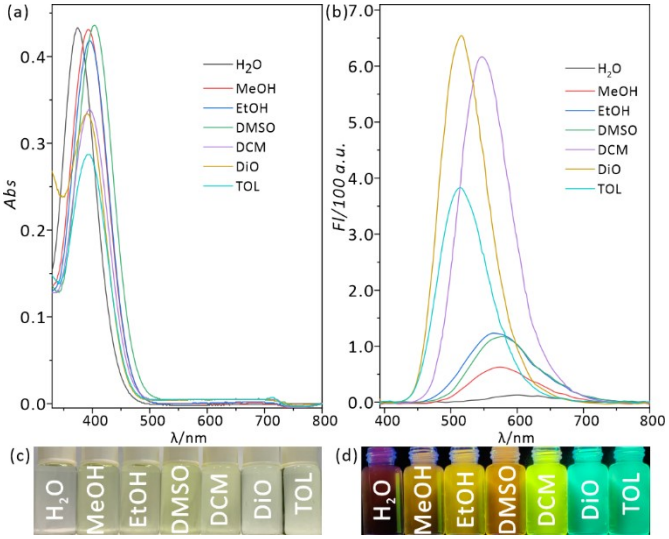

Fig. S2 Spectral properties of dye **1c** (10 μM) in different solvents. (a) UV-visible absorption spectrogram; (b) Fluorescence emission spectrogram (λ_{ex} = 383 nm, slit widths: 3 nm/3 nm); (c) photographs in daylight; (d) UV photographs under a 365 nm lamp and darkroom.

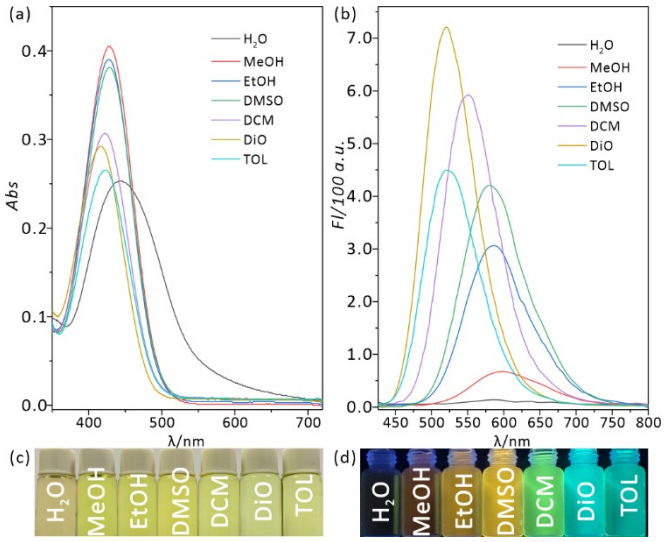

Fig. S3 Spectral properties of dye **1d** (10 μM) in different solvents. (a) UV-visible absorption spectrogram; (b) Fluorescence emission spectrogram (λ_{ex} = 416 nm, slit widths: 3 nm/3 nm); (c) photographs in daylight; (d) UV photographs under a 365 nm lamp and darkroom.

Table S1. Spectral properties of dyes **1b**-**1d** in diverse solvents.

Dyes	Solvents	Δf [a]	$\lambda_{Abs,max}$ /nm	$\lambda_{Em,max}$ /nm	Stokes shift /nm	ε [b]	Φ [c] /%
1b	H_2O	0.3200	447	–	–	1.05	–
	MeOH	0.3092	417	602	185	3.60	2.19
	EtOH	0.2887	416	575	159	3.54	19.26
	DMSO	0.2642	412	560	148	3.41	23.56
	DCM	0.2170	415	545	130	3.20	60.77
	DiO	0.0205	408	503	95	3.18	53.89
	TOL	0.0153	411	495	84	2.61	42.40
1c	H_2O	0.3200	375	604	229	4.33	1.28
	MeOH	0.3092	394	575	181	4.31	5.12
	EtOH	0.2887	395	570	175	4.18	10.34
	DMSO	0.2642	405	574	169	4.36	8.64
	DCM	0.2170	396	545	149	3.39	30.04
	DiO	0.0205	390	516	126	3.34	48.08
	TOL	0.0153	391	514	123	2.87	53.27
1d	H_2O	0.3200	445	–	–	2.53	1.08
	MeOH	0.3092	429	599	170	4.05	5.55
	EtOH	0.2887	428	583	155	3.90	14.88
	DMSO	0.2642	427	581	154	3.81	23.45
	DCM	0.2170	422	550	128	3.07	39.86
	DiO	0.0205	415	520	105	2.92	42.83
	TOL	0.0153	421	519	98	2.65	42.18

[a] the Lippert Mataga polarity parameter.

[b] $\times 10^4$ $M^{-1}cm^{-1}$.

[c] Coumarin-153 (Φ = 0.547 in ethanol) was used as the reference compound.

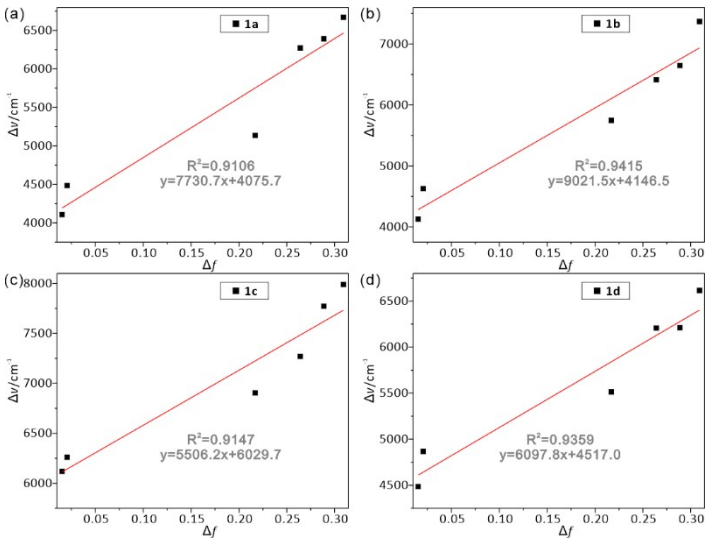

Fig. S4 The Stokes shifts (Δ*v*) of **1a**-**1d** as a function of orientational polarizability (Δ*f*) in distinct solvents.

The Lippert-Mataga equation:

$$\Delta v = v_a - v_e = \frac{2\Delta\mu^2}{hca^3}\Delta f + constant \quad (1)$$

$$\Delta\mu = \mu_E - \mu_G \quad (2)$$

$$\Delta f = \frac{\varepsilon - 1}{2\varepsilon + 1} - \frac{n^2 - 1}{2n^2 + 1} \quad (3)$$

where Δv is the Stokes shift, v_a and v_e represent the maximum absorption and the emission wavenumbers (cm^{-1}), respectively, $\Delta\mu$ is the transition dipole moments between the ground (μ_E) and the excited (μ_G) states, h is Planck's constant, c is the speed of light, and a corresponds to the Onsager cavity radius; Δf is the orientation polarizability of solvents, ε and n are the dielectric constant (ε) and refractive index (n), respectively.

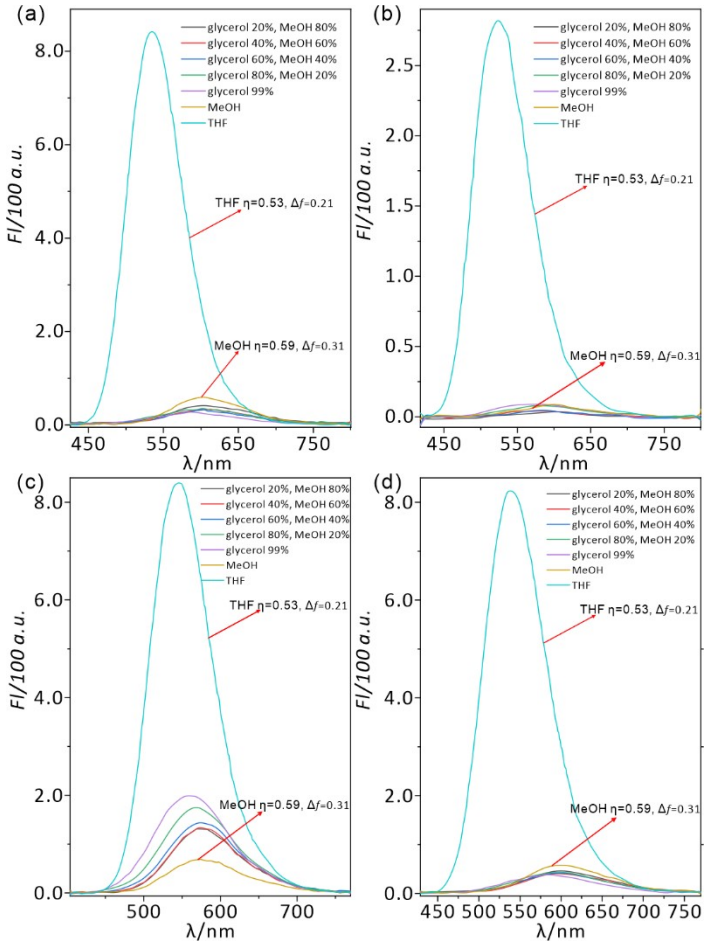

Fig. S5 The fluorescence emission of dyes **1a** (a), **1b** (b), **1c** (c) and **1d** (d) (10 μM) in MeOH/glycerol mixture under different viscosity, THF and MeOH. THF and MeOH have almost the same viscosity (0.53 cP vs 0.59 cP) while distinct polarity (0.21 vs 0.31).

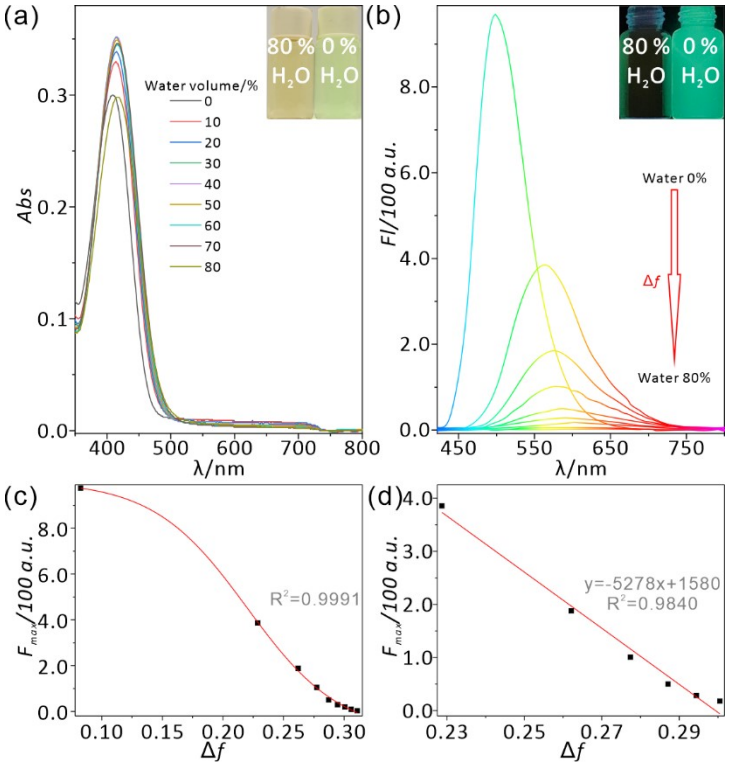

Fig. S6 Spectral properties of dye **1b** (10 μM) in DiO/H_2O with the increasing polarity (water volume from 0 % to 80 %). (a) UV-visible absorption spectrogram; (b) emission spectrogram (λ_{ex} = 412 nm, slit widths: 5 nm/1.5 nm); (c) Curvilinear relationship between the F_{max} and Δ*f* in the range from 0.0826 (0 % H_2O) to 0.3108 (80 % H_2O); (d) Linear relationship between the F_{max} and Δ*f* (range from 0.2287 (10 % H_2O) to 0.3005 (60 % H_2O)).

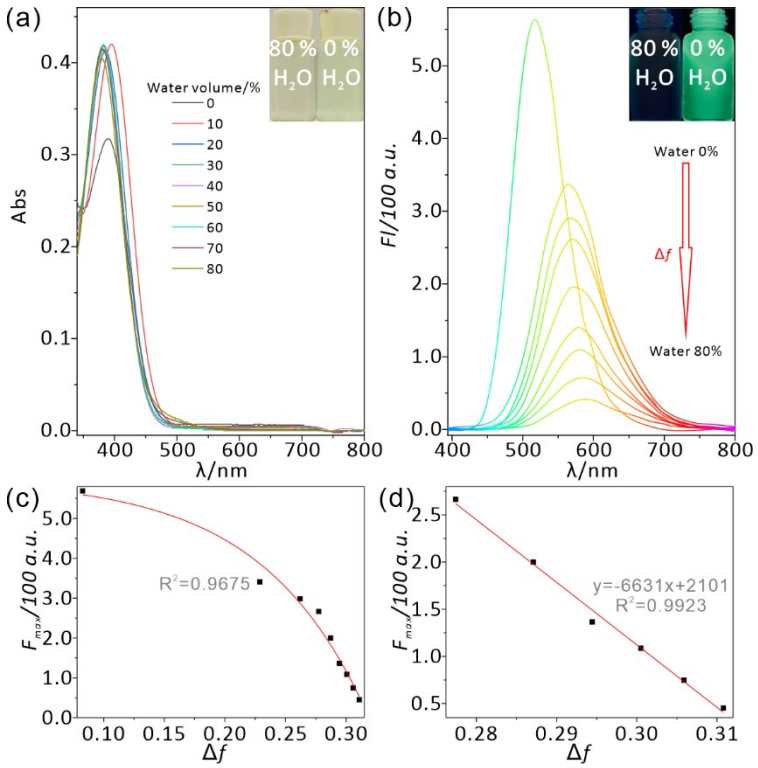

Fig. S7 Spectral properties of dye **1c** (10 μM) in DiO/H_2O with the increasing polarity (water volume from 0 % to 80 %). (a) UV-visible absorption spectrogram; (b) emission spectrogram (λ_{ex} = 384 nm, slit widths: 3 nm/3 nm); (c) Curvilinear relationship between the F_{max} and Δf in the range from 0.0826 (0 % H_2O) to 0.3108 (80 % H_2O); (d) Linear relationship between the F_{max} and Δf (range from 0.2774 (30 % H_2O) to 0.3108 (80 % H_2O)).

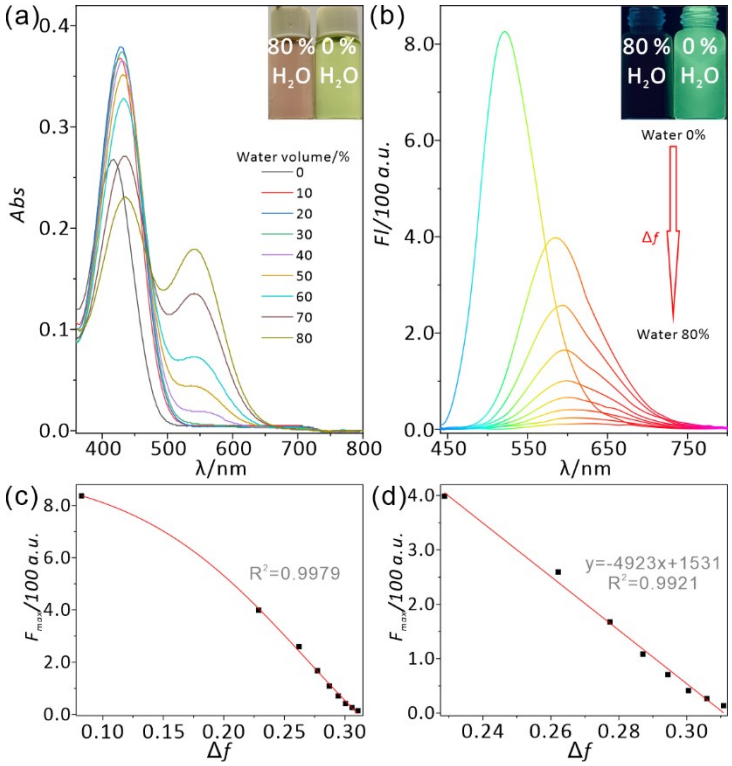

Fig. S8 Spectral properties of dye **1d** (10 μM) in DiO/H_2O with the increasing polarity (water volume from 0 % to 80 %). (a) UV-visible absorption spectrogram; (b) emission spectrogram (λ_{ex} = 431 nm, slit widths: 3 nm/3 nm); (c) Curvilinear relationship between the F_{max} and the Δf in the range from 0.0826 (0 % H_2O) to 0.3108 (80 % H_2O); (d) Linear relationship between the F_{max} and Δf (range from 0.2287 (10 % H_2O) to 0.3108 (80 % H_2O)).

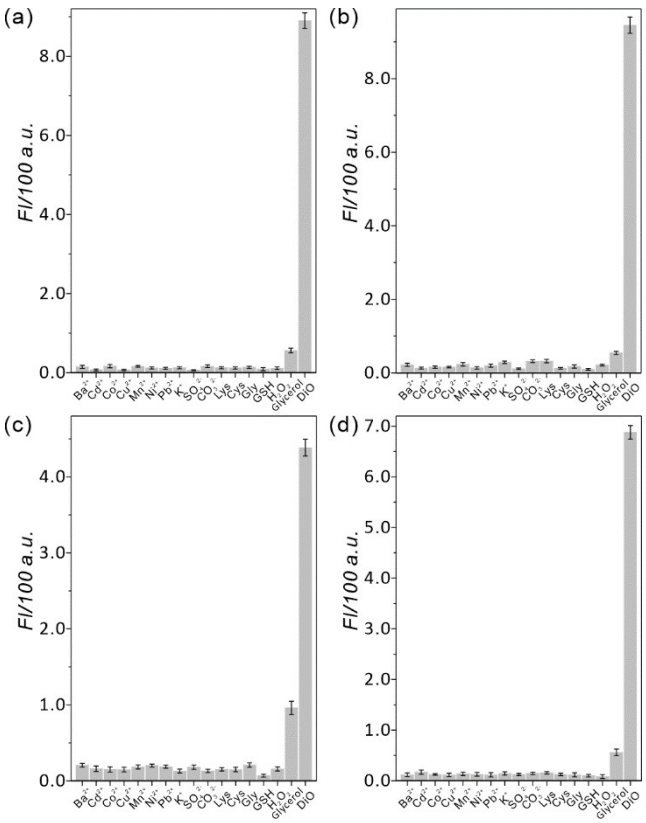

Fig. S9 Fluorescence intensity of dyes **1a** (a), **1b** (b), **1c** (c), **1d** (d) (10 μM) towards other interfering ions and biomolecules (1 mM) in double-distilled water containing 10 % DMSO. The data were shown as mean ± SD (n = 3).

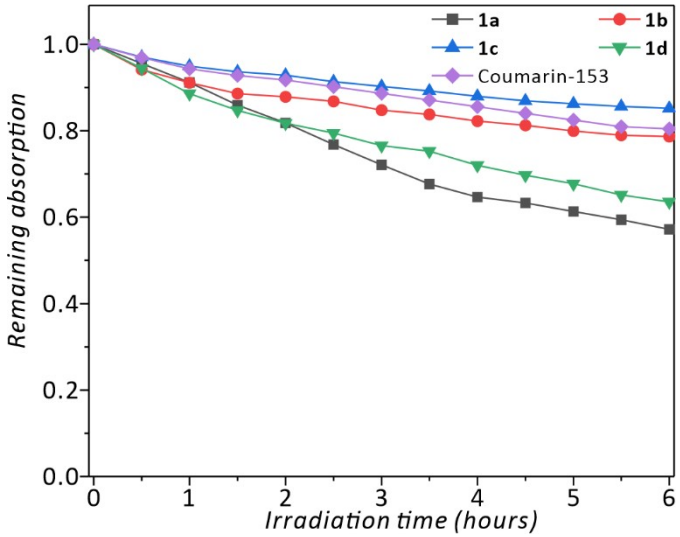

Fig. S10 Photostability of dyes **1a**-**1d** (10 μM) in acetonitrile reflecting by the variation trend of remaining absorption for 6 h.

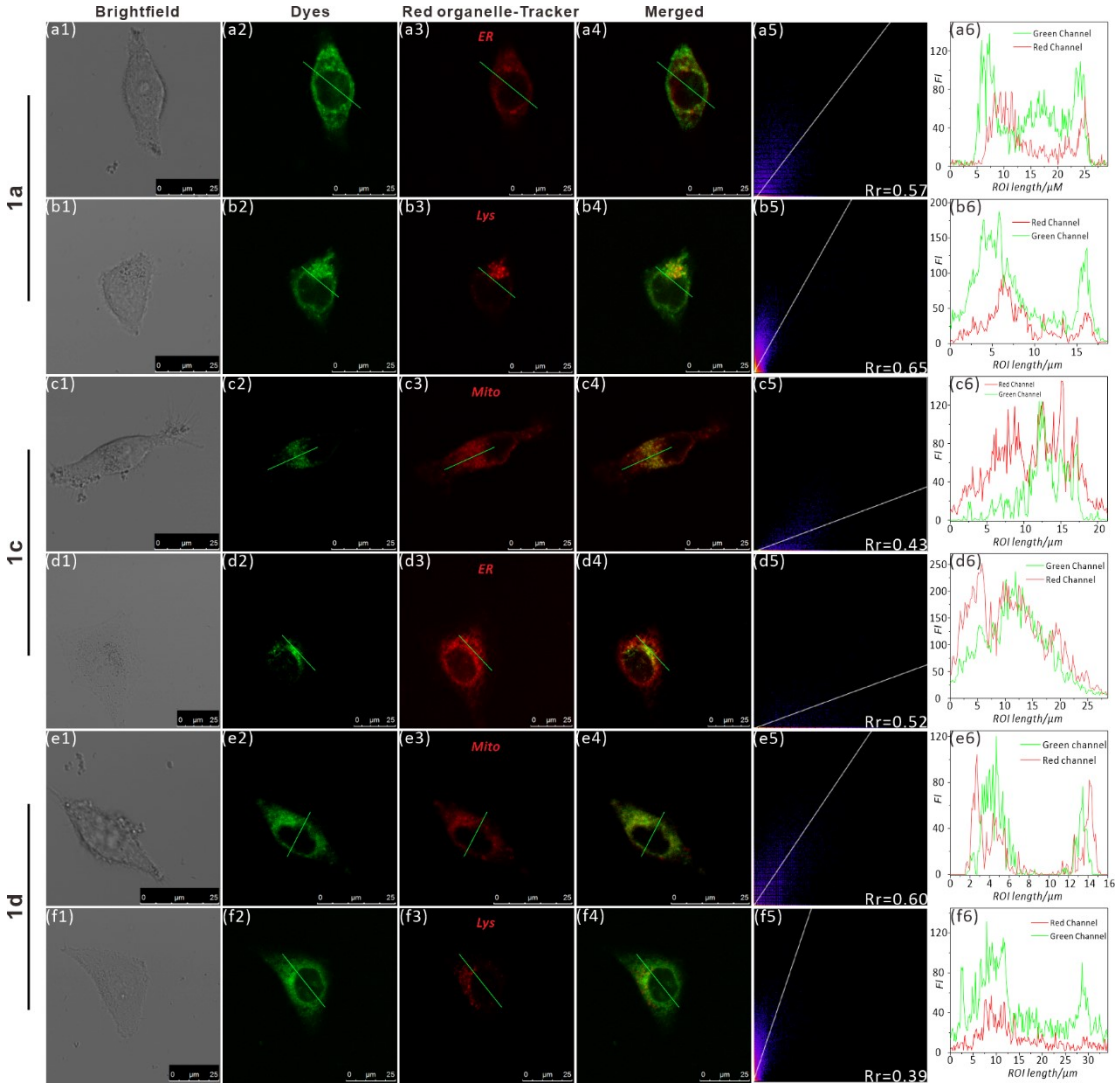

Fig S11 Fluorescence confocal images of HeLa cells with dye **1a** (5 μM), **1c** (5 μM) and **1d** (5 μM). (a1, b1, c1, d1, e1, f1) The brightfield images of HeLa cells; (a2, b2, c2, d2, e2, f2) Confocal images (green channel) of HeLa cells with **1a**, **1c** and **1d**, respectively; (a3, b3, c3, d3, e3, f3) Confocal images (Red channel) of HeLa cells with Red ERTracker (1 μM), Red LysTracker (1 μM) and Mito Tracker Red CMXRos (1 μM), respectively; (a4, b4, c4, d4, e4, f4) The merged images of green channel and red channel; (a5, b5, c5, d5, e5, f5) The fluorescence intensity correlation plot; (a6, b6, c6, d6, e6, f6) Intensity profiles of the regions of interest (ROIs) in the green channel and red channel.

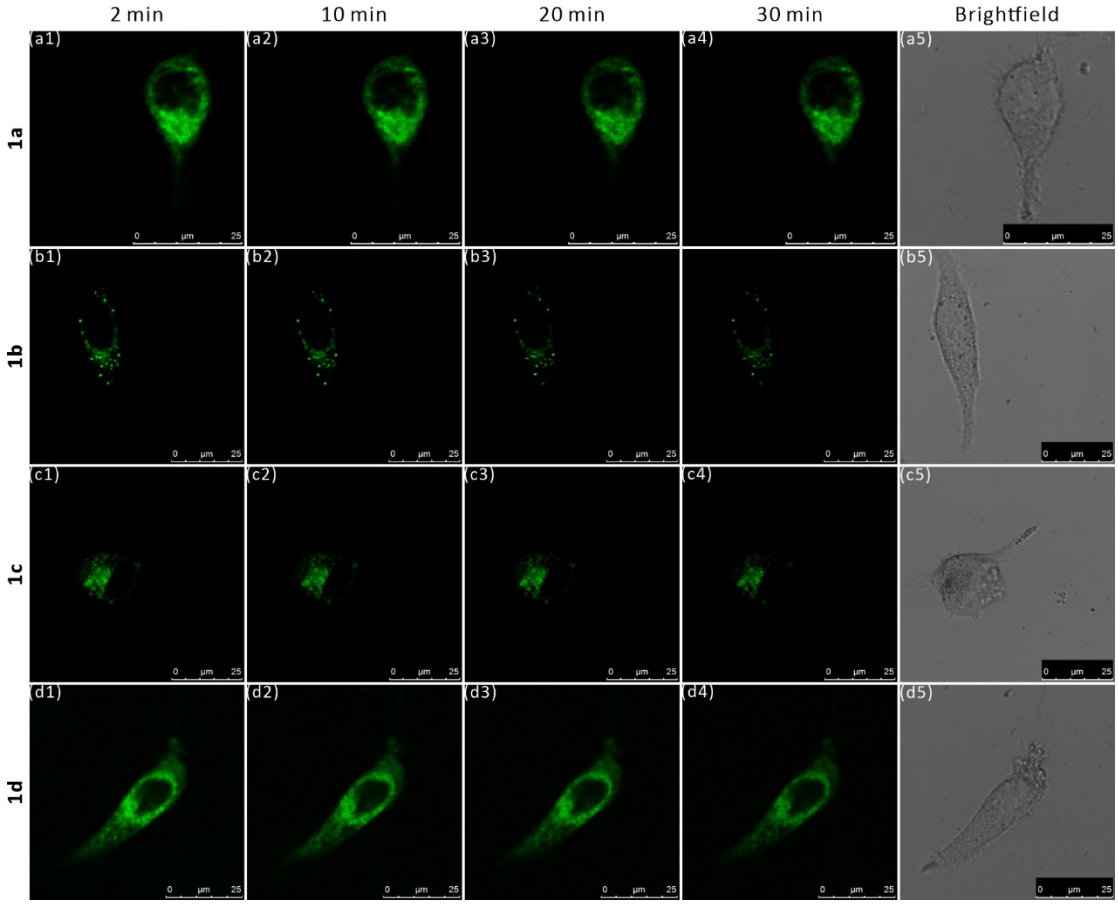

Fig S12 Photobleaching experiments of dyes **1a**-**1d** (5 μM). (a1-a4, b1-b4, c1-c4, d1-d4) The cell images of **1a**-**1d** after laser irradiation for different time in HeLa cells. (a5, b5, c5, d5) The brightfield images of HeLa cells.

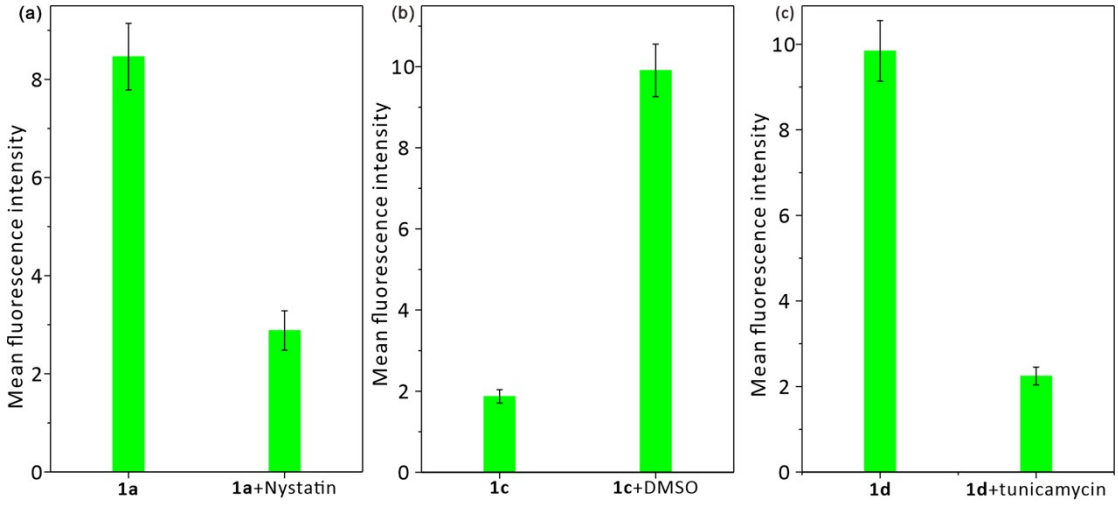

Fig. S13 Mean fluorescence intensity of living HeLa cells incubated with dyes **1a** (a), **1c** (b) and **1d** (c) (10 μM) before and after adding the drugs including nystatin (10 μM), DMSO (10 μL) or tunicamycin (500 μg/mL). The data were shown as mean ± SD (n = 3).

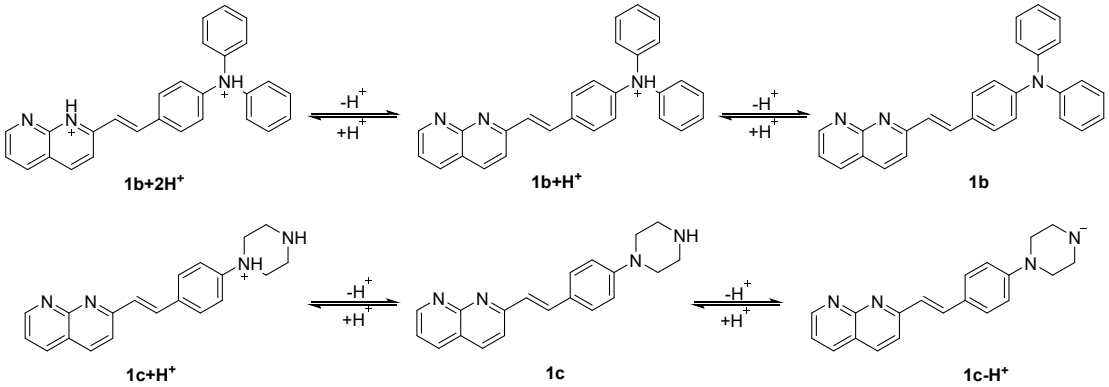

Scheme S2. Protonated-deprotonated processes of derivatives **1b** and **1c**.

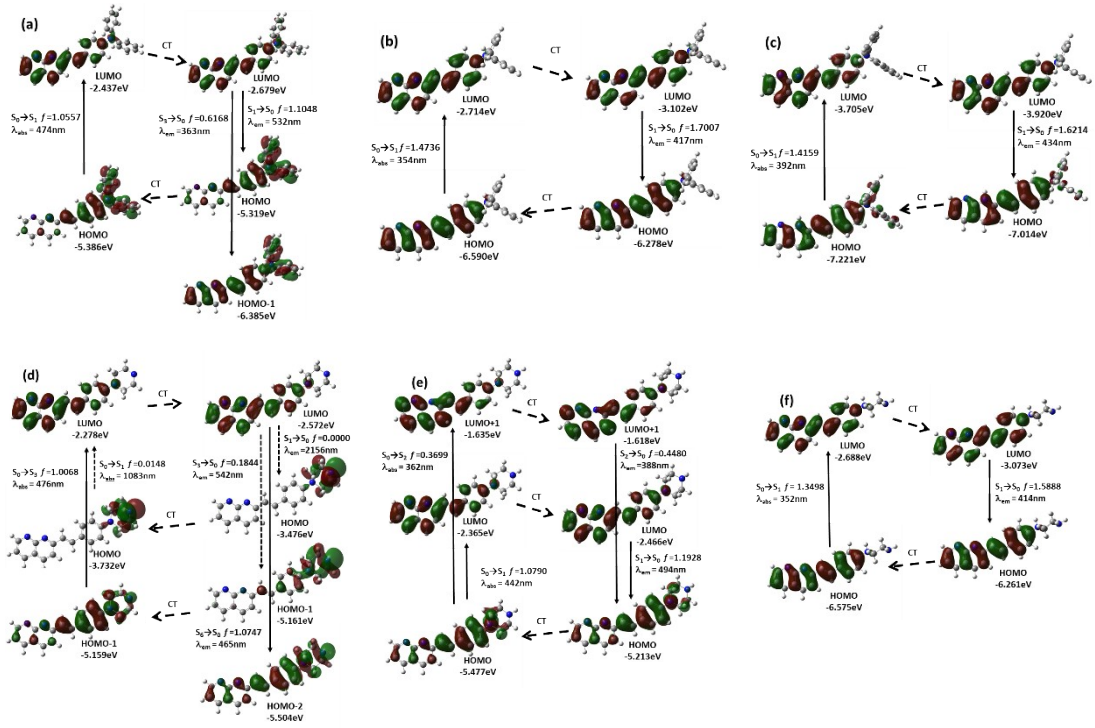

Fig. S14 The frontier molecular orbitals (FMOs) involved in the vertical excitation(left) and emission(right) of derivatives **1b**-**1c** and their protonated or deprotonated forms from B3LYP/6-31G+(d) computations in water medium (PCM). (a) **1b**, (b) **1b**+H^+, (c) **1b**+$2H^+$, (d) **1c**-H^+, (e) **1c**, (f) **1c**+H^+. CT stands for conformation transformation. Excitation and radiative processes are marked as solid lines and the non-radiative processes are marked by dotted lines.

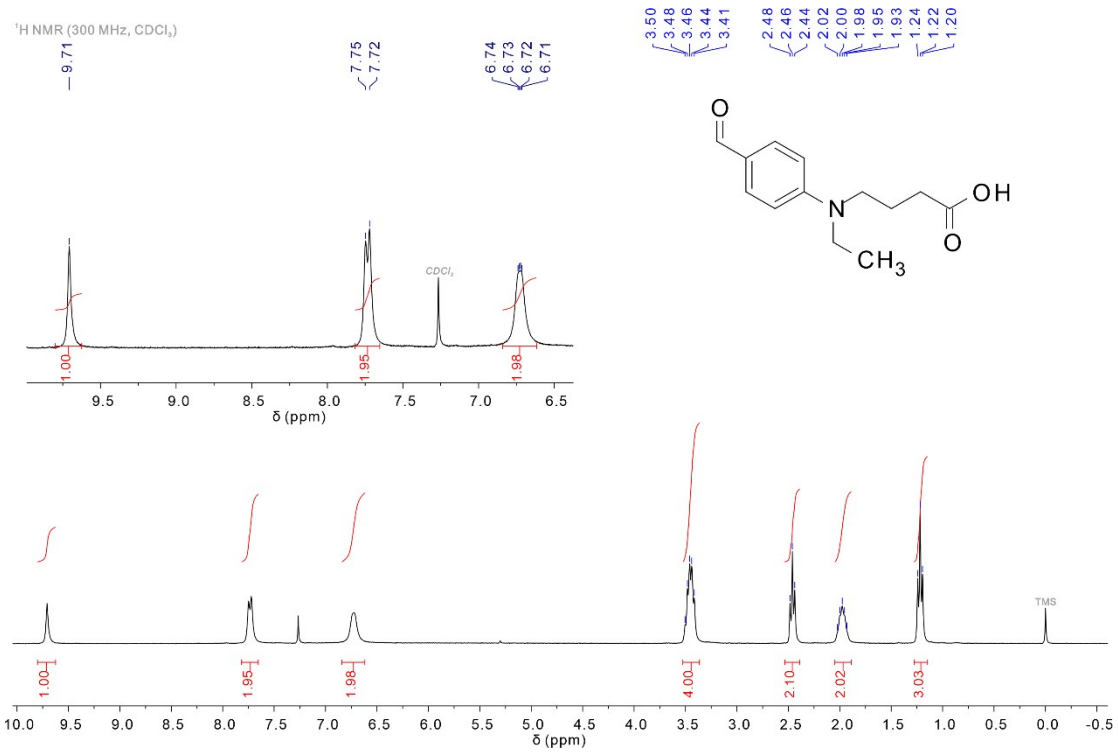

Fig. S15 ^{1}H NMR spectrum of compound **4d** (300 MHz, $CDCl_3$).

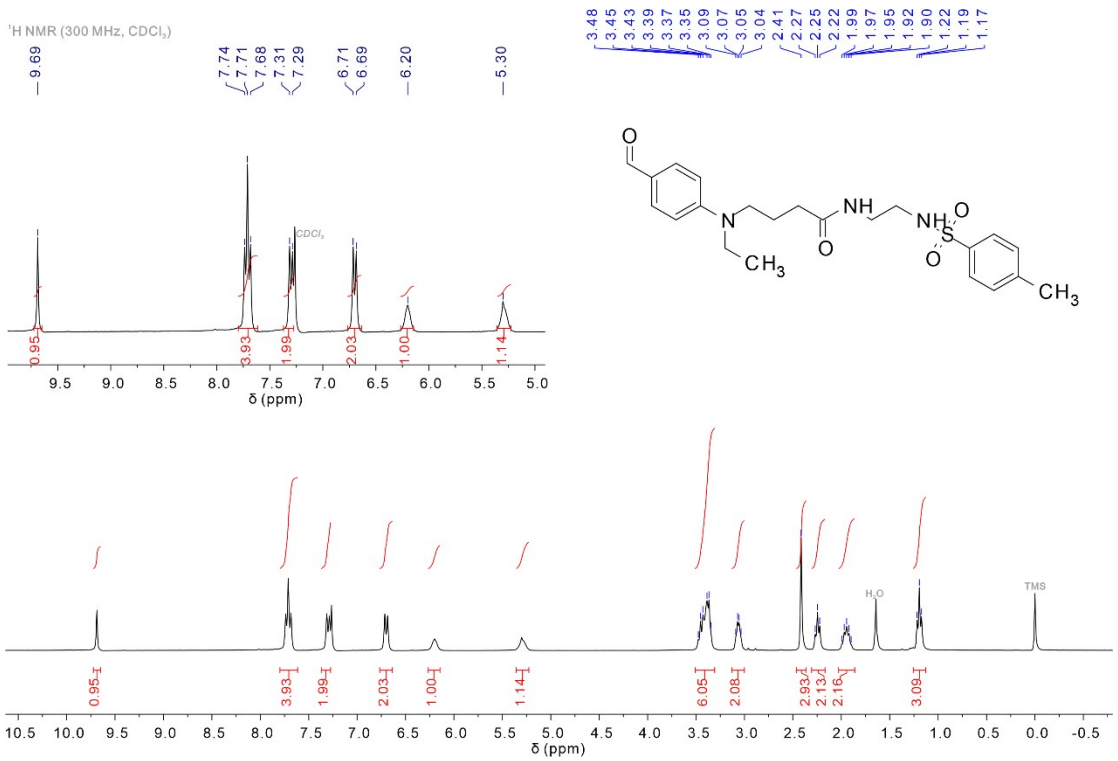

Fig. S16 ^{1}H NMR spectrum of compound **2d** (300 MHz, $CDCl_3$).

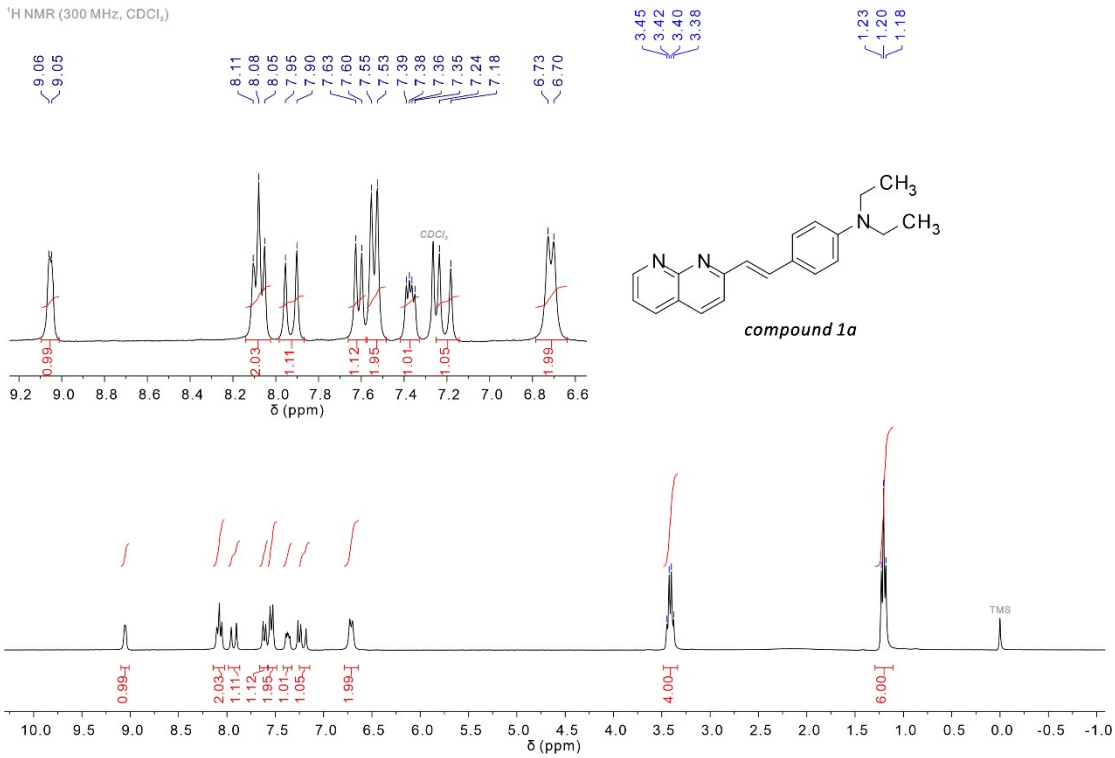

Fig. S17 ^{1}H NMR spectrum of compound **1a** (300 MHz, $CDCl_3$).

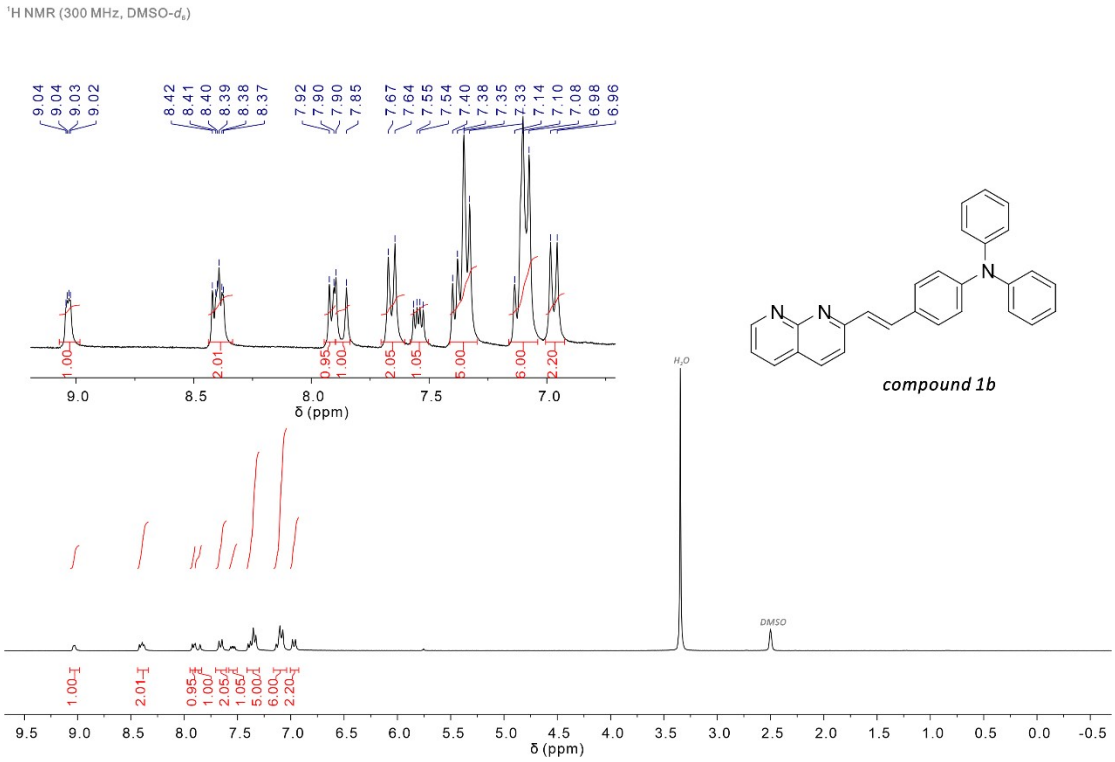

Fig. S18 ^{1}H NMR spectrum of compound **1b** (300 MHz, DMSO-d_6).

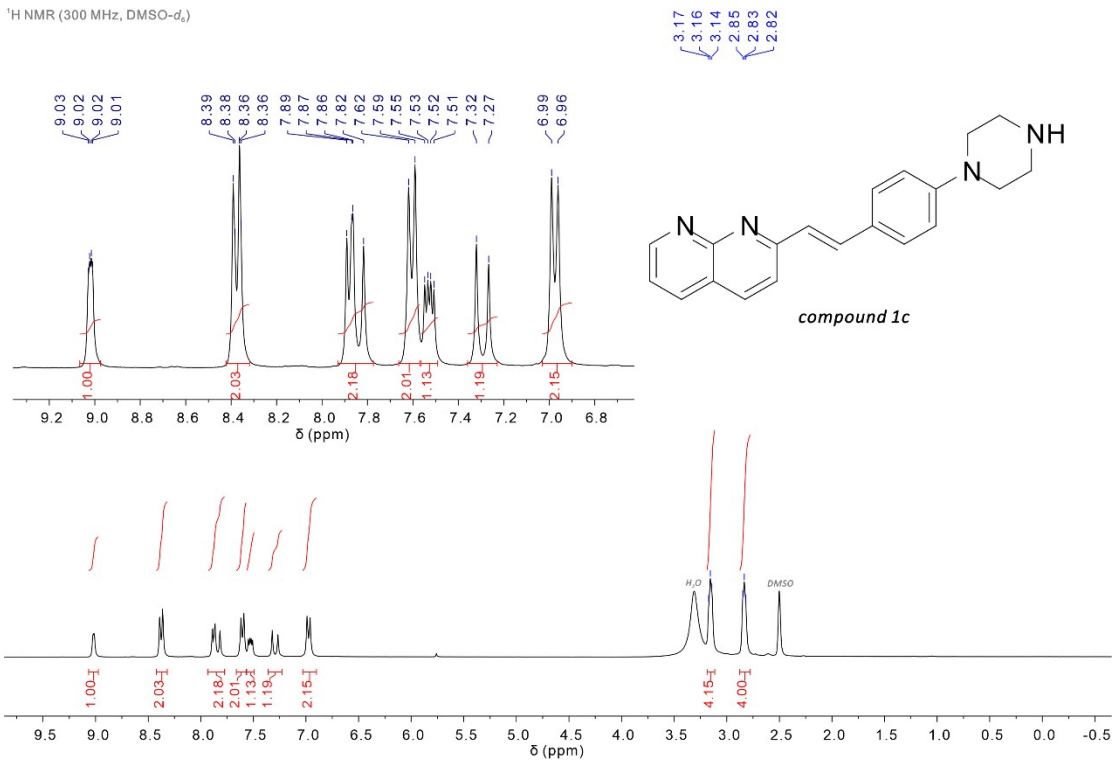

Fig. S19 ^{1}H NMR spectrum of compound **1c** (300 MHz, DMSO-d_6).

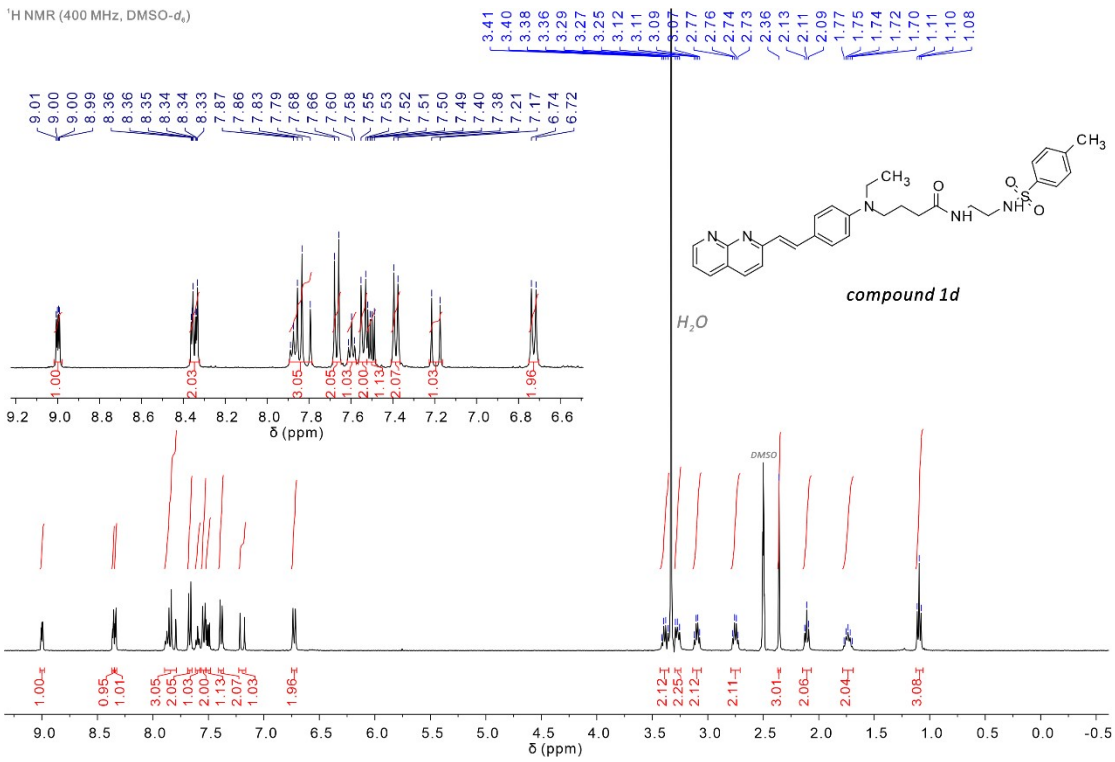

Fig. S20 ^{1}H NMR spectrum of compound **1d** (400 MHz, DMSO-d_6).

Acquisition Parameter

Source Type	ESI	Ion Polarity	Positive	Set Nebulizer	0.6 Bar
Focus	Active	Set Capillary	4500 V	Set Dry Heater	180 °C
Scan Begin	50 m/z	Set End Plate Offset	-500 V	Set Dry Gas	4.0 l/min
Scan End	1500 m/z	Set Collision Cell RF	250.0 Vpp	Set Divert Valve	Waste

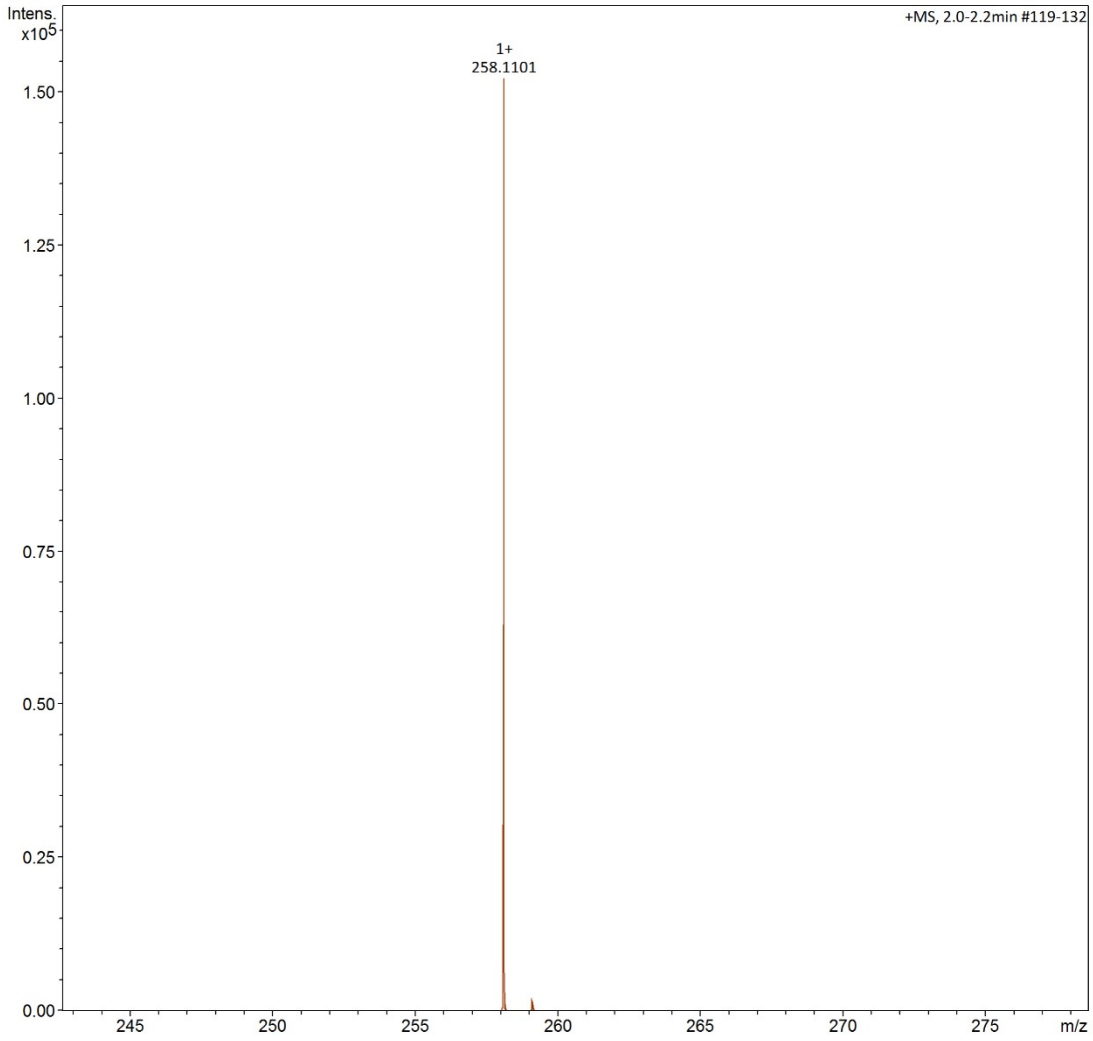

Fig. S21 HRMS (ESI^+) spectrum of compound **4d**.

Acquisition Parameter

Source Type	ESI	Ion Polarity	Positive	Set Nebulizer	0.6 Bar
Focus	Active	Set Capillary	4500 V	Set Dry Heater	180 °C
Scan Begin	50 m/z	Set End Plate Offset	-500 V	Set Dry Gas	4.0 l/min
Scan End	1500 m/z	Set Collision Cell RF	250.0 Vpp	Set Divert Valve	Waste

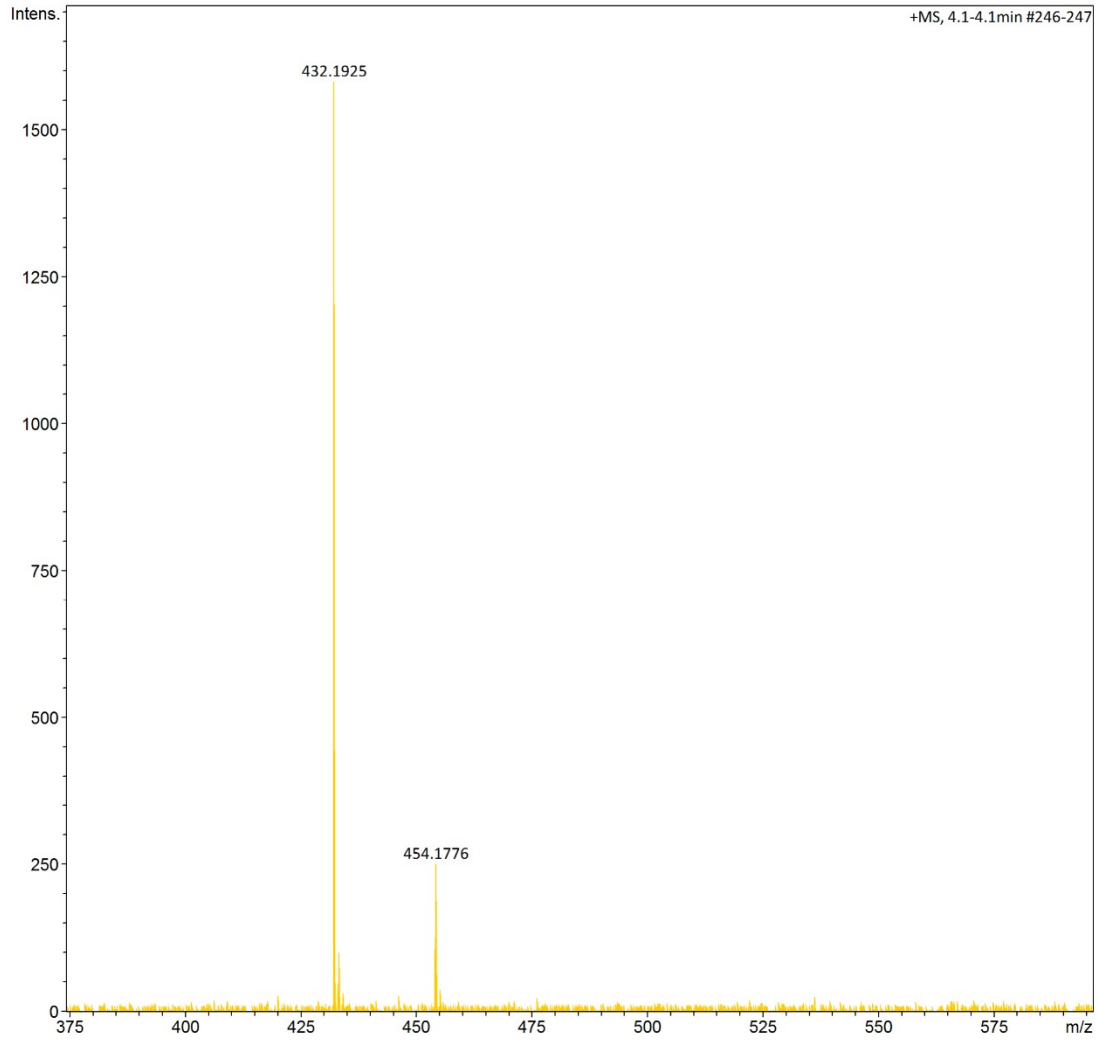

Fig. S22 HRMS (ESI$^+$) spectrum of compound **2d**.

Acquisition Parameter

Source Type	ESI	Ion Polarity	Positive	Set Nebulizer	0.6 Bar
Focus	Active	Set Capillary	4500 V	Set Dry Heater	180 °C
Scan Begin	50 m/z	Set End Plate Offset	-500 V	Set Dry Gas	4.0 l/min
Scan End	1500 m/z	Set Collision Cell RF	250.0 Vpp	Set Divert Valve	Waste

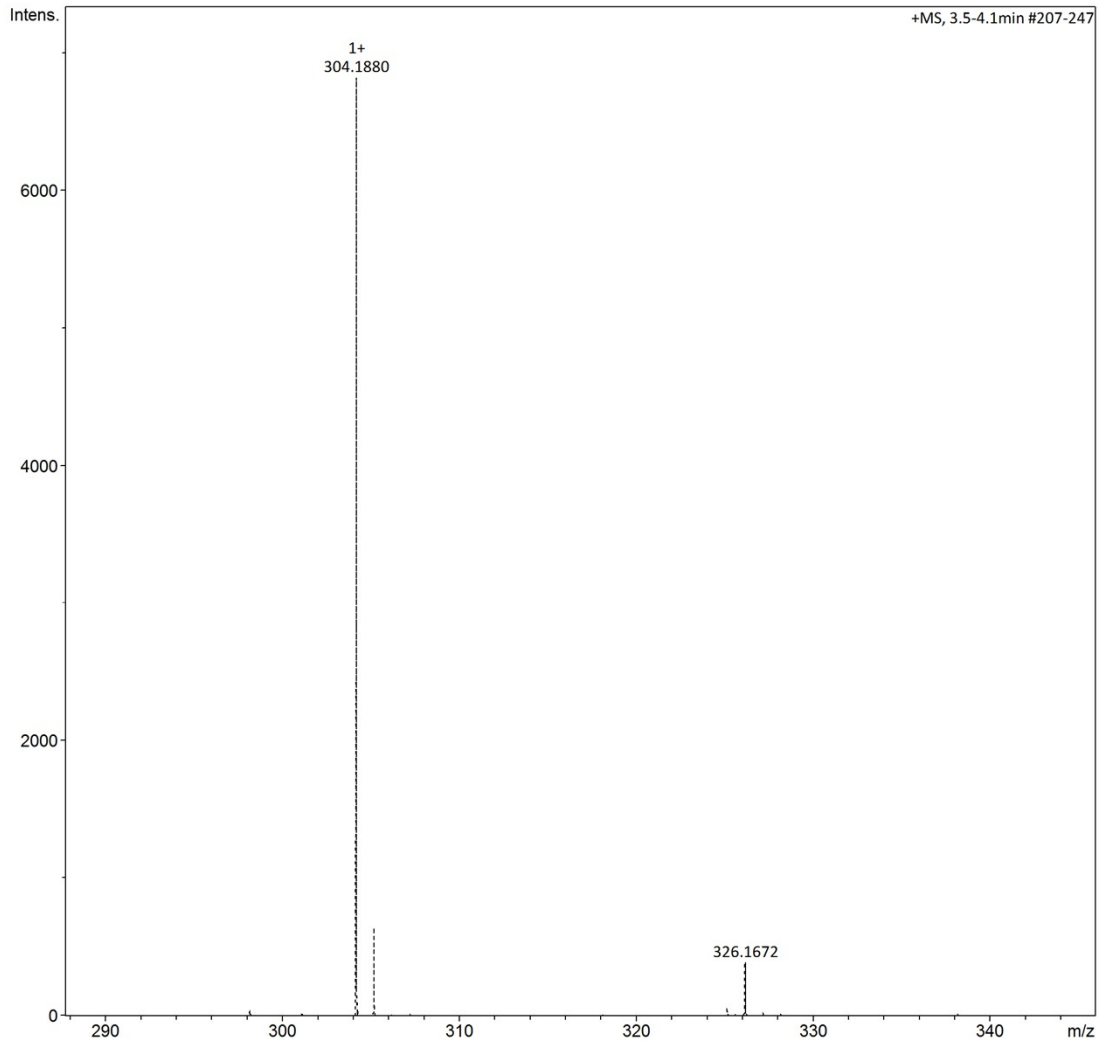

Fig. S23 HRMS (ESI$^+$) spectrum of compound **1a**.

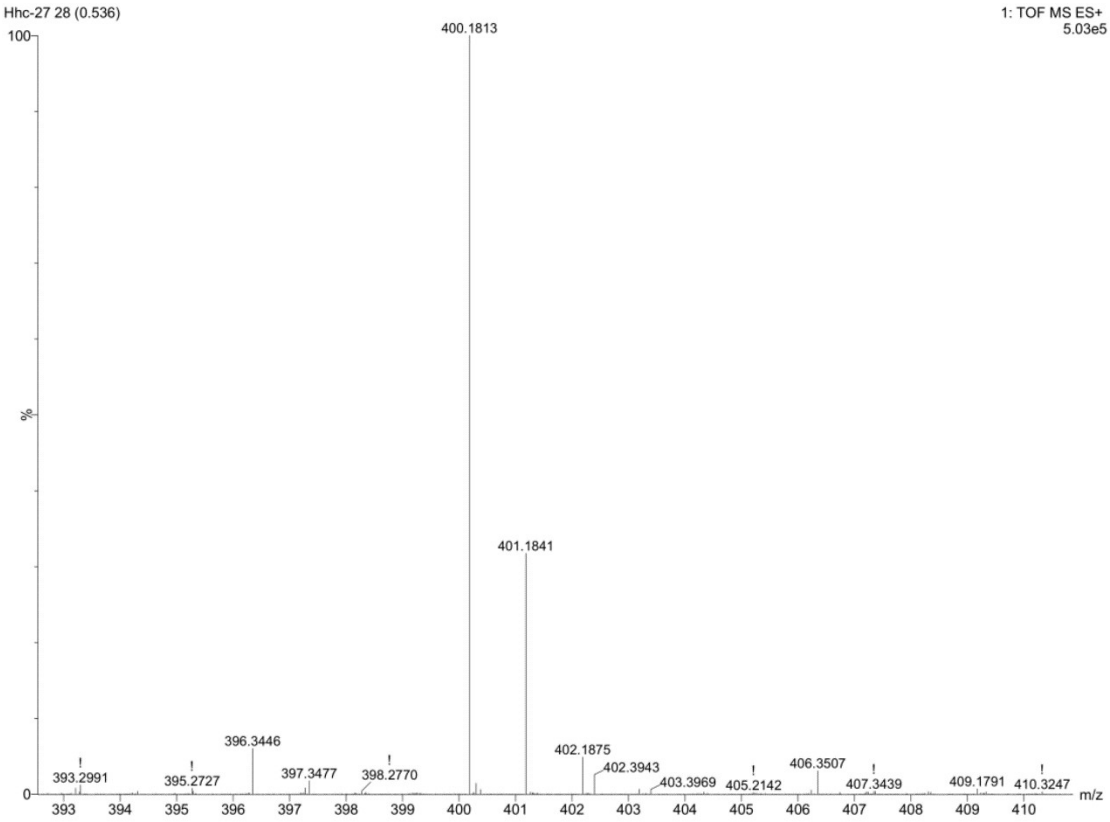

Fig. S24 HRMS (ESI$^+$) spectrum of compound **1b**.

Acquisition Parameter

Source Type	ESI	Ion Polarity	Positive	Set Nebulizer	0.6 Bar
Focus	Active	Set Capillary	4500 V	Set Dry Heater	180 °C
Scan Begin	50 m/z	Set End Plate Offset	-500 V	Set Dry Gas	4.0 l/min
Scan End	1500 m/z	Set Collision Cell RF	250.0 Vpp	Set Divert Valve	Waste

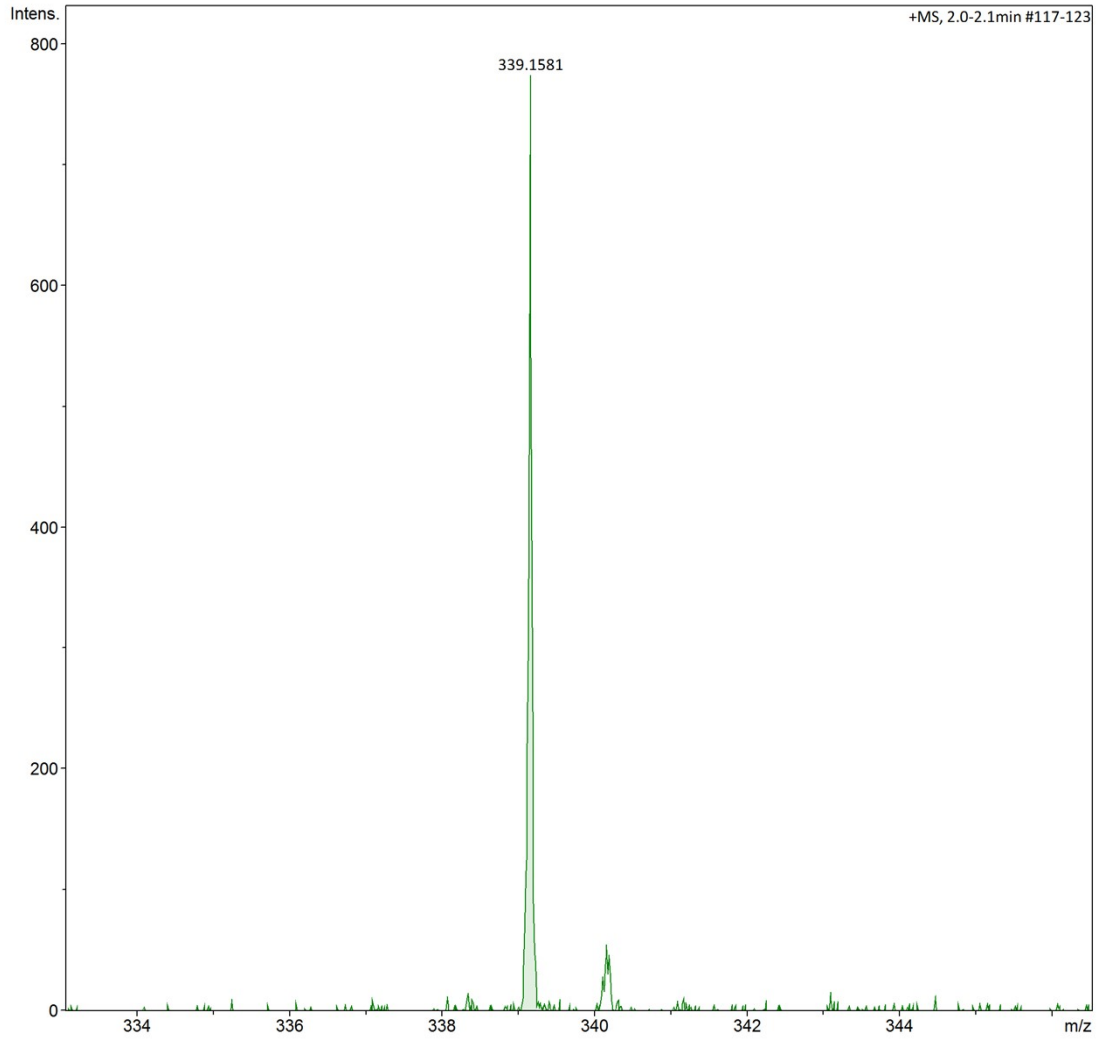

Fig. S25 HRMS (ESI^+) spectrum of compound **1c**.

Acquisition Parameter

Source Type	ESI	Ion Polarity	Positive	Set Nebulizer	0.6 Bar
Focus	Active	Set Capillary	4500 V	Set Dry Heater	180 °C
Scan Begin	50 m/z	Set End Plate Offset	-500 V	Set Dry Gas	4.0 l/min
Scan End	1500 m/z	Set Collision Cell RF	250.0 Vpp	Set Divert Valve	Waste

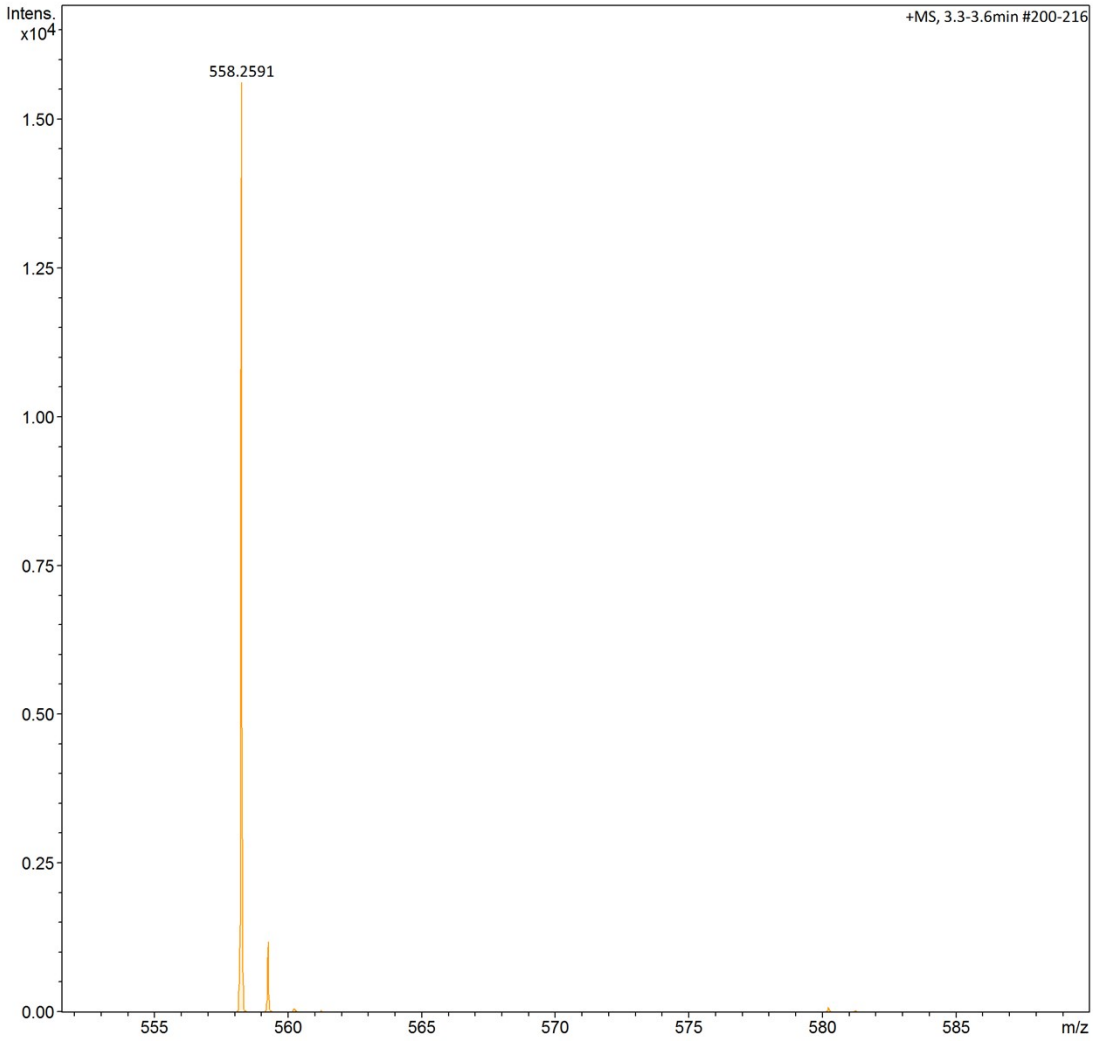

Fig. S26 HRMS (ESI^+) spectrum of compound **1d**.

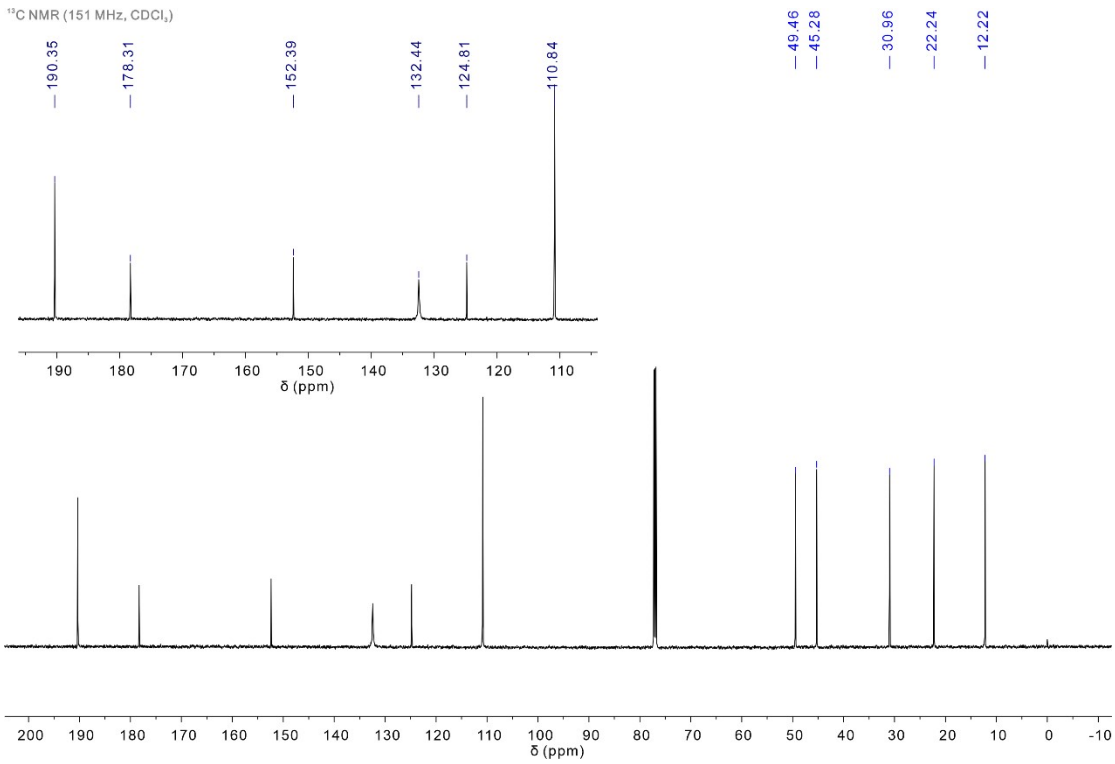

Fig. S27 ^{13}C NMR spectrum of compound **4d** (151 MHz, $CDCl_3$).

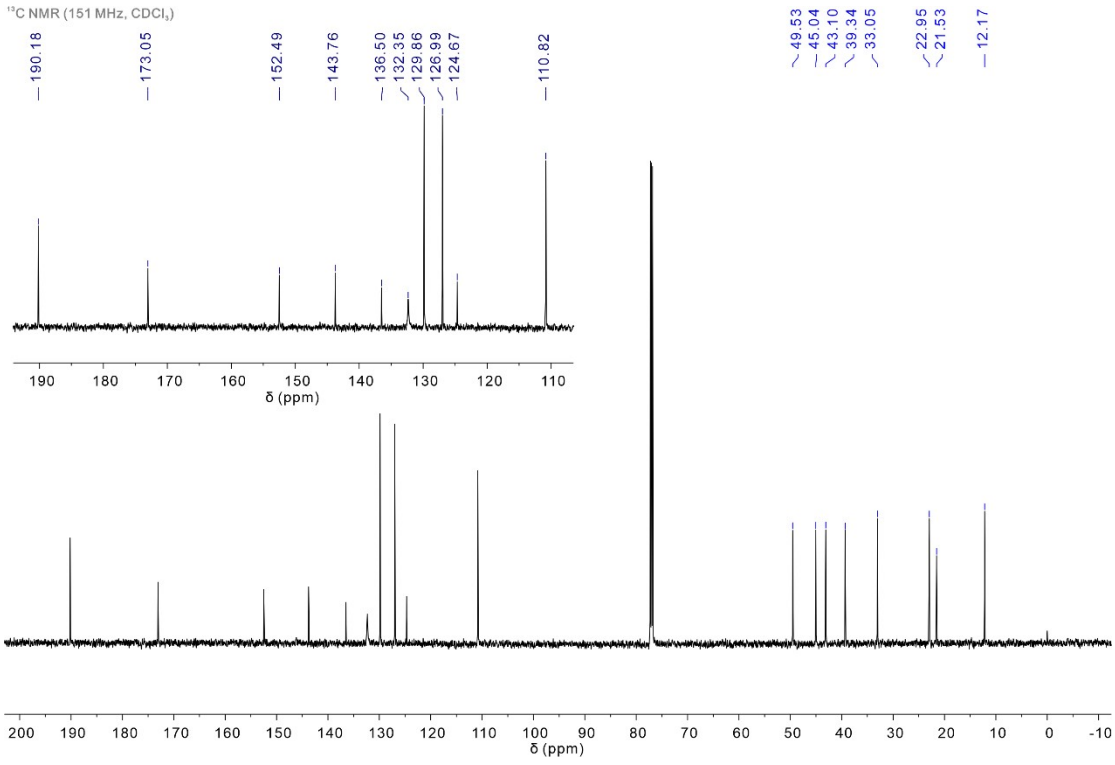

Fig. S28 ^{13}C NMR spectrum of compound **2d** (151MHz, $CDCl_3$).

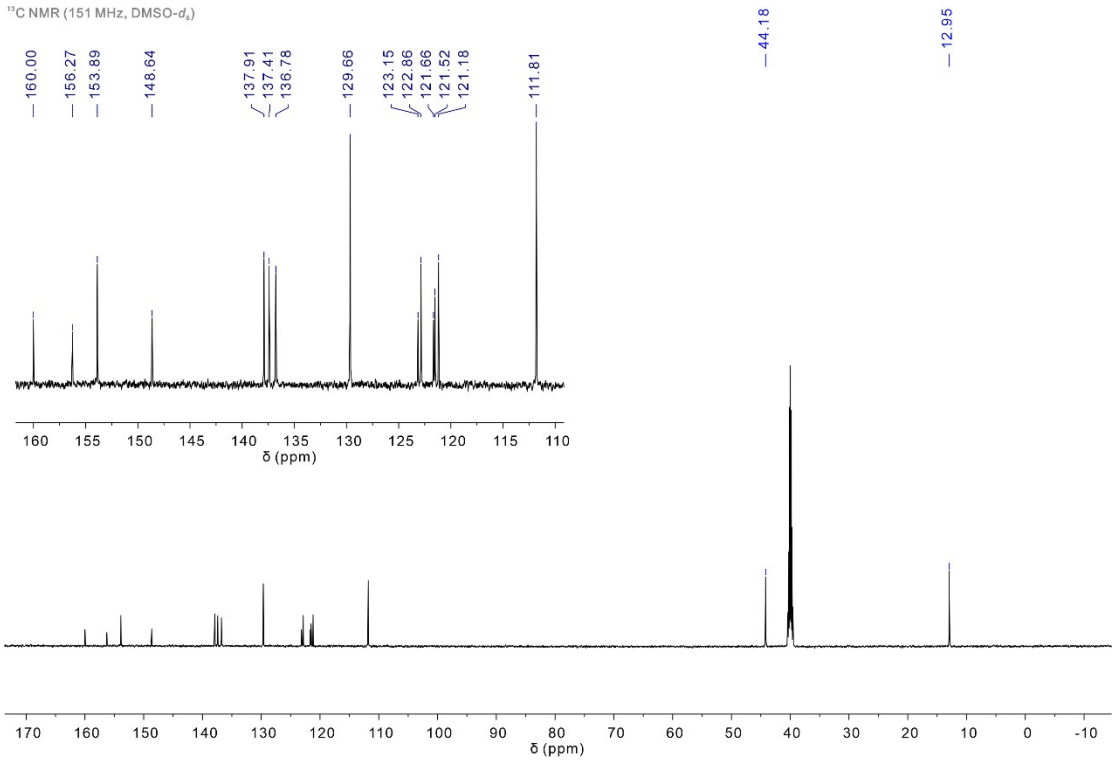

Fig. S29 ^{13}C NMR spectrum of compound **1a** (151MHz, DMSO-d_6).

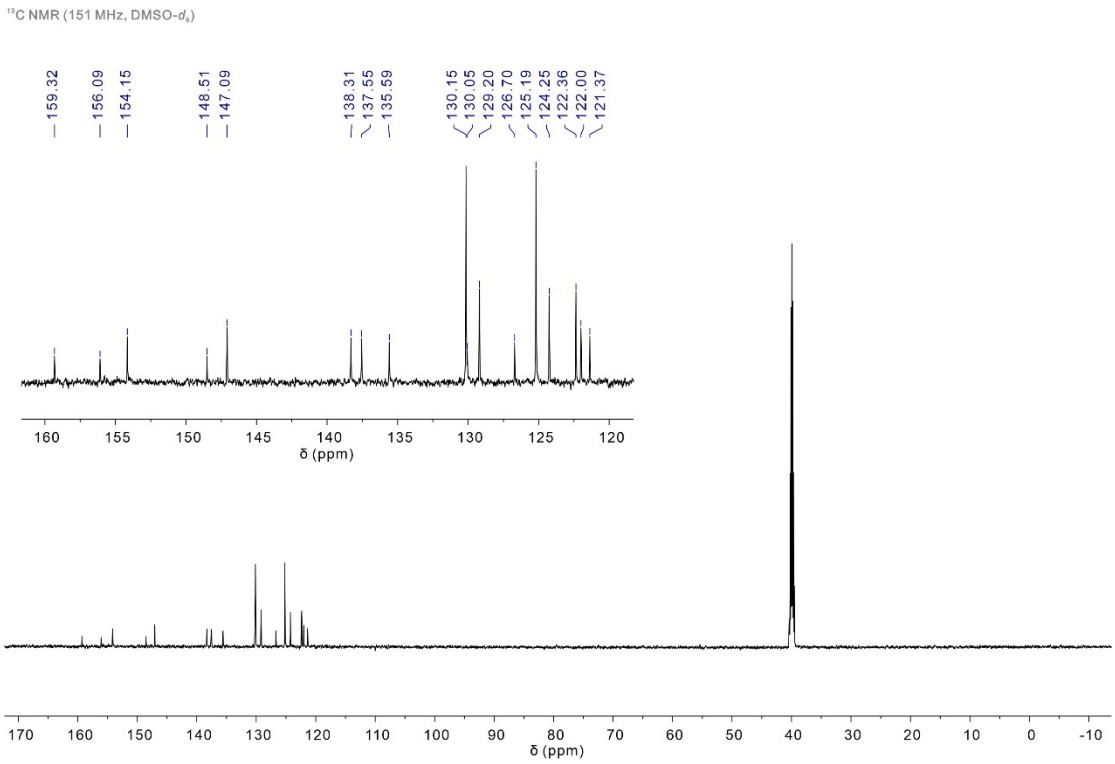

Fig. S30 ^{13}C NMR spectrum of compound **1b** (151MHz, DMSO-d_6).

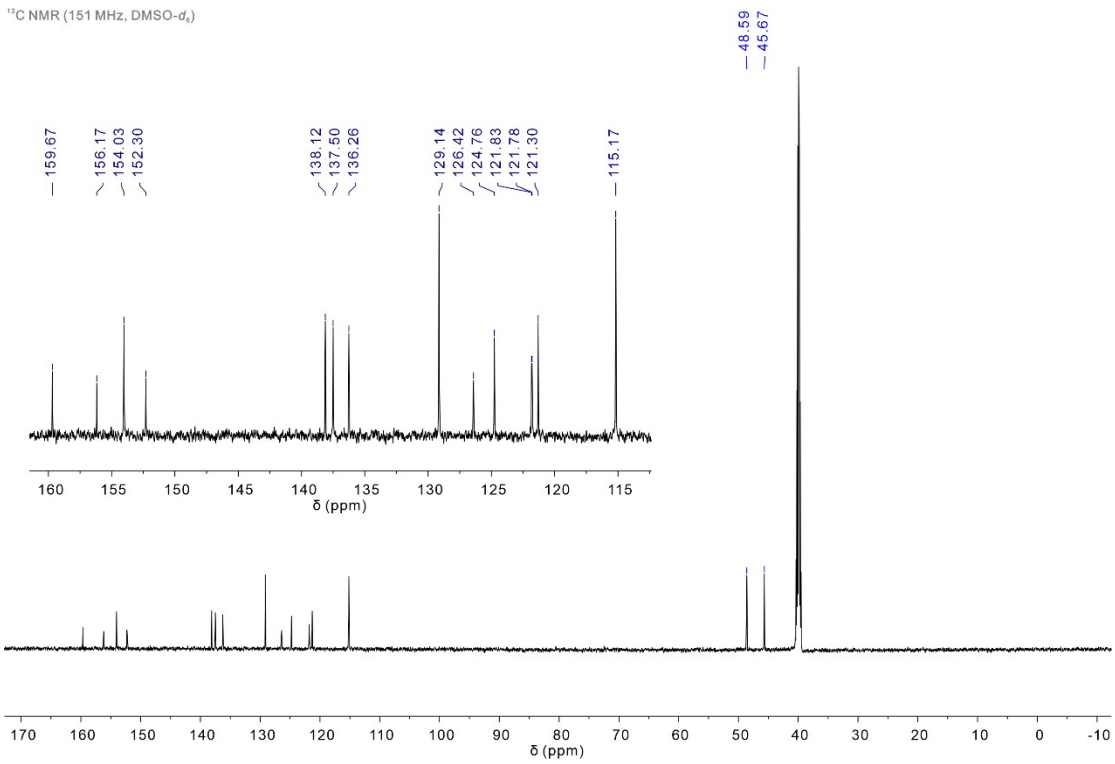

Fig. S31 ^{13}C NMR spectrum of compound **1c** (151MHz, DMSO-d_6).

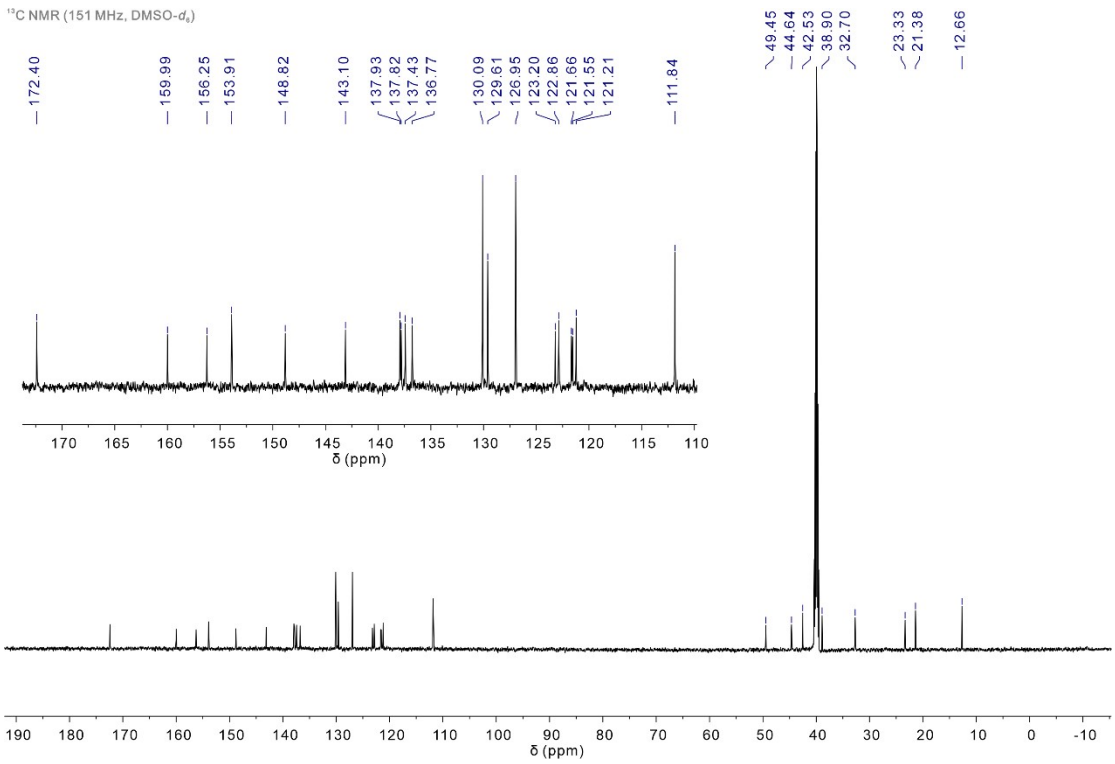

Fig. S32 ^{13}C NMR spectrum of compound **1d** (151MHz, DMSO-d_6).